The Journal of Chemical Physics

Energetics and kinetics of ethylbenzene adsorption on epitaxial FeO(111) and $Fe_3O_4(111)$ films studied by thermal desorption and photoelectron spectroscopy

Cite as: J. Chem. Phys. **108**, 9506 (1998); https://doi.org/10.1063/1.476421
Submitted: 15 December 1997 . Accepted: 04 March 1998 . Published Online: 01 June 1998

D. Zscherpel, W. Ranke, W. Weiss, and R. Schlögl

Energetics and kinetics of ethylbenzene adsorption on epitaxial FeO(111) and Fe_3O_4(111) films studied by thermal desorption and photoelectron spectroscopy

D. Zscherpel, W. Ranke, W. Weiss,[a] and R. Schlögl
Fritz-Haber-Institut der Max-Planck-Gesellschaft, Faradayweg 4-6, D-14195 Berlin, Germany

(Received 15 December 1997; accepted 4 March 1998)

The adsorption of ethylbenzene (EB) has been studied on thin films of FeO(111) and Fe_3O_4(111) grown epitaxially on Pt(111) using thermal desorption spectroscopy (TDS), ultraviolet photoelectron spectroscopy (UPS) and low energy electron diffraction (LEED). Applying a threshold analysis of the TDS data, desorption energies E_{des} and the corresponding frequency factors are deduced. The UPS measurements are performed under adsorption–desorption equilibrium conditions: The spectra are taken at varying sample temperature at constant EB gas phase pressures. From the spectra, the EB-coverages Θ_{EB} are deduced. From the adsorption isobars obtained in this way, isosteric heats of adsorption $q_{st}(\Theta_{EB})$ are obtained which are compared to the desorption energies E_{des} deduced from TDS. On the oxygen-terminated FeO(111) surface, two adsorption states are observed, a physisorbed first layer (β-EB) followed by condensation (α-EB). Their UP spectra are almost identical and very similar to the spectrum of gas phase EB. On Fe_3O_4(111), a more strongly chemisorbed species (γ_1-EB) is adsorbed first, followed by physisorbed β- and condensed α-EB. The chemisorbed phase exhibits a strong shift and split of the highest occupied π orbitals of the phenyl group. This indicates a strong interaction between the substrate and the adsorbed molecules that are adsorbed with the phenyl ring lying flat on the surface. The desorption energies E_{des} and the isosteric heats of adsorption q_{st}, respectively, are 91 (85) kJ/mol for γ_1-, 55 (58) kJ/mol for β- and 50 (52) kJ/mol for α-EB and agree generally well. The differences are discussed in terms of different coverage ranges accessible for both methods, the nonequilibrium character of the TDS method and to the threshold analysis which yields only data for the most loosely bound molecules desorbing first in each desorption track. © *1998 American Institute of Physics.* [S0021-9606(98)50522-3]

I. INTRODUCTION

The technical dehydrogenation of ethylbenzene (EB) to styrene is an important synthesis reaction. It is carried out over iron oxide based catalysts in an EB-steam mixture at temperatures around 600 °C. Lee[1] and Hirano[2,3] performed detailed studies on the kinetics of the synthesis reaction and on the dependence of the catalyst activity on the partial pressures of EB, styrene and water. Muhler *et al.*[4,5] investigated the nature of the active catalyst. Goodman *et al.*[6,7] studied the kinetics of unpromoted and potassium promoted iron oxide catalysts under model conditions by infrared and Auger electron spectroscopy. These model catalysts were prepared by oxidizing the surface region of a polycrystalline iron disk. It has been shown in the measurements that for both promoted and unpromoted samples the apparent activation energies are the same indicating identical active sites on these surfaces.

In a former work[8] ultrathin iron oxide films of different stoichiometry were grown onto Pt(111) substrates and were investigated with thermal desorption spectroscopy (TDS). The experiments showed several desorption peaks on the different films which were assigned to different adsorption sites. The condensed multilayer of EB desorbs at 155 K. Peaks observed at higher temperature were assigned to weakly chemisorbed EB. Upon high exposures and formation of condensed EB multilayers an additional broad desorption signal was observed at higher temperatures which coincide for Fe_2O_3 films with the reaction temperature (870 K) of the technical iron oxide catalyst. In stationary mass spectroscopic measurements it was shown that only Fe_2O_3 films are active for the dehydrogenation of EB. However, the order of the films could not be controlled in these measurements because no LEED system was available.

In this work we investigate the adsorption of EB on FeO and Fe_3O_4 films in more detail comparing results using TDS and ultraviolet photoelectron spectroscopy (UPS). In the UPS measurements, the EB coverage can be derived both from the adsorbate photoemission signal and from the attenuation of the substrate emission by the adsorbate overlayer. As in a recent study of NH_3 adsorption on Ge surfaces,[9] the UPS measurements are performed in adsorption–desorption equilibrium, i.e., the stationary coverage $\Theta(p,T)$ is measured as a function of pressure and temperature. From these data, isosteric heats of adsorption $q_{st}(\Theta)$ can be derived which can be compared with desorption energies deduced from the TDS measurements.

[a]Author to whom correspondence should be addressed. Electronic mail: weiss_w@fhi-berlin.mpg.de

II. EXPERIMENT

A. Sample holder and preparation

As described previously,[10] the iron oxide layers were prepared epitaxially on Pt(111) samples by cyclic evaporation of iron followed by oxidation. The oxides of different stoichiometry can easily be distinguished by their LEED patterns.[10] The Pt substrates were clamped by tungsten wires and molybdenum screws onto the sapphire sample holder. A NiCr–Ni thermocouple was spot-welded to the Pt substrate. Its contact to the manipulator was achieved using screws and contact springs of the same thermocouple material. The arrangement is described in detail elsewhere.[11]

A closed FeO(111) film up to 2 or 3 Fe–O-bilayers thick forms upon evaporation of Fe in portions of less than a monolayer (ML) each oxidized for about 3 min at 1020 K in 10^{-6} mbar oxygen. When more than 2–3 ML are deposited, the FeO layer does not grow further but instead quite small and high Fe_3O_4 islands are formed.[12]

A closed Fe_3O_4(111) layer can be prepared by depositing a thick iron layer ($\geqslant$10 Fe ML) in one run onto the FeO(111) layer and oxidizing it for a longer time (10–20 min) at 870 K. In this way island formation is avoided. The layer can be grown thicker by further evaporation–oxidation cycles. It is stable even upon annealing up to 1020 K. Before each measurement, the layer was reoxidized in 10^{-6} mbar oxygen at 1020 K.

Depending of the precise preparation conditions (thickness of deposited Fe, oxidation time, oxidation temperature), the order of the surfaces varies. The degree of order was controlled qualitatively by monitoring the spot width and the spot to background intensity ratio in LEED. In this work we only show results on well ordered films

Ethylbenzene from a sure sealed bottle (ALDRICH) under N_2 atmosphere was sucked under vacuum into a small glass bulb supply filled with activated molecular sieve in order to reduce the level of possible water contamination. The EB vapor from the tube between this supply and the leak valve was pumped off before each experiment to remove any possible accumulated contaminants. The ionization probability of EB is by a factor of about 7 higher than for N_2.[13] The pressure indication of the ionization gauge was corrected by this factor.

B. Thermal desorption spectroscopy (TDS)

The measurements were performed in a vacuum chamber with a base pressure of 2×10^{-10} mbar. It was equipped with a display LEED optics with video camera and digital image processing, a quadrupole mass spectrometer (QMS) with computer control, sample preparation facilities (Ar^+-sputter gun, iron evaporator), ion gauge, gas inlet system, and sample transfer system. The chamber is described in detail elsewhere.[11]

In the TDS experiments, EB was adsorbed onto the sample at 100 K. Exposures ε are given in Langmuir units with 1 L$=1.33\times10^{-6}$ mbar s. The heating rate was always 5 K/s. Variations of the QMS sensitivity were accounted for by setting equal the total desorbing amount after condensation of 10 L EB. This is based on the assumption that the sticking coefficient for condensation is constant and independent of the substrate surface.

C. Ultraviolet photoelectron spectroscopy (UPS)

Photoelectron spectroscopic measurements were performed in a separate UPS chamber equipped with a double-pass cylindrical mirror analyser (CMA, Physical Electronics), a He resonance lamp (He I line 21.2 eV, He II line 40.8 eV), a high resolution Henzler-type[14] LEED system suitable for spot profile analysis (SPA-LEED), Ar^+-sputter gun, iron evaporator and gas inlet system. The base pressure was about 5×10^{-11} mbar.

For sample rotation, a differentially pumped feedthrough was used which allowed to use a tube as manipulator shaft which can directly be filled with liquid N_2 for cooling. In order to set the sample to a certain temperature, a certain amount of liquid N_2 (usually in steps of 10 to 30 g) was filled in. After about 3 min, the N_2 is evaporated and thermal equilibrium established. The thermal drift during the following 3 min necessary for taking a spectrum was always less than 3 K. The mean value of initial and final temperature during taking a spectrum was used as reference temperature. The advantage of this method of temperature adjustment is that no parts are much colder than the sample and no condensation occurs on the manipulator except when also the sample temperature approaches the condensation temperature. The pressure sink of a condensing surfaces is avoided and the pressure distribution in the chamber remains homogeneous.

For the determination of the isosteric heat of adsorption $q_{st}(\Theta)$, at least three adsorption isobars $\Theta(T)_{p=\text{const.}}$ had to be measured in one run in order to minimize instrumental sensitivity changes. The coverage Θ was deduced from the UP spectra as described below. First, the clean surface spectrum was taken several times to be sure that the spectrometer sensitivity was constant. Then the EB pressure p_{EB} was set to 4×10^{-9} mbar, a spectrum was taken, the sample cooled by one step, a spectrum taken, cooled one step, etc. When the strongly increasing EB coverage indicated transition to condensation, cooling was stopped and p_{EB} increased to 4×10^{-8} mbar. Now spectra were taken during stepwise warming the sample. Finally, p_{EB} was set to 4×10^{-7} mbar and another run made again with stepwise decreasing T. The total time necessary was 4 to 7 h. Contamination by residual gases (water, CO, H_2) was not noticed. The reason is that the oxide surfaces are quite unreactive towards these gases and EB adsorption is always dominating.

Above about 400 K, slight changes in the shape of the spectra indicated beginning decomposition. After prolonged heating, the background in the spectra increased slightly. This affected the coverage determination and the measurements were therefore limited to $T<370$ K.

In order to keep the short-time spectrometer sensitivity constant it turned out to be important to take spectra in equal time intervals (6 min in our case) throughout the whole run. Long time sensitivity changes of up to 4% within 7 h could not be avoided. How they were considered is described in the results section.

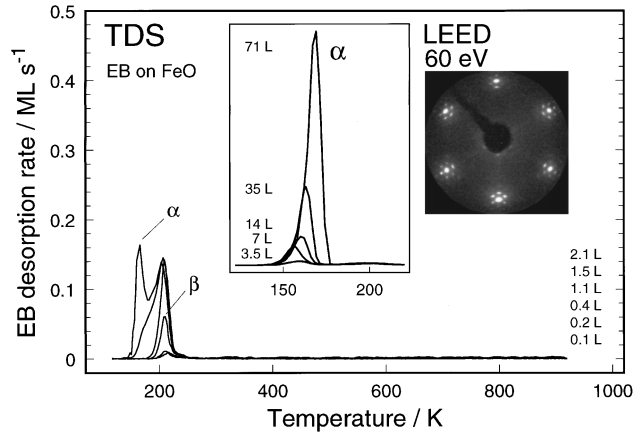

FIG. 1. Thermal desorption spectra of ethylbenzene (EB) from a 1–2 ML thick FeO(111) film on Pt(111) after exposure to the indicated amounts in Langmuir units (1 L=1.33×10^{-6} mbar s) at 100 K; β: physisorbed EB; α: condensed EB. The LEED pattern is from the clean film, $E_p=60$ eV.

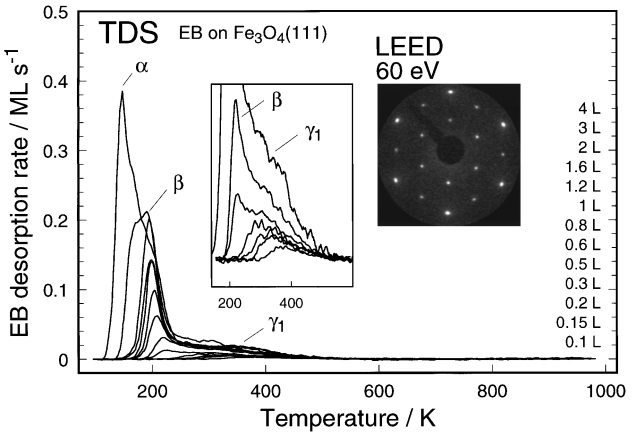

FIG. 2. Thermal desorption spectra of ethylbenzene (EB) from a thick $Fe_3O_4(111)$ film on Pt(111) after exposure to the indicated amounts (1 L=1.33×10^{-6} mbar s) at 100 K; γ_1: chemisorbed EB; β: physisorbed EB; α: condensed EB. The LEED pattern is from the clean film, $E_p=60$ eV.

Even after an irradiation of the sample covered with ethylbenzene over a period of 5 h with He I or He II radiation, no indication of a beam-induced change of the adsorbate spectra could be detected. UPS can thus be considered as a nondestructive method for this system.

III. RESULTS

A. Thermal desorption spectroscopy

Figure 1 shows the TDS spectra of EB after exposure of the FeO(111) film to varying amounts. At low exposures only one desorption peak at 210 K is observed. The desorption follows a first order kinetics.[8] The intensity increases up to 1.3 L where the species labelled β-EB saturates. We define this saturation coverage as 1 monolayer (ML). Upon higher exposures an additional EB species α is observed which starts to desorb at 155 K. The insert shows that it desorbs with a common leading edge for different initial coverages. It thus follows a zero order kinetics and corresponds to condensed EB.[8] The β species is only slightly more strongly bound and we call it physisorbed EB. The inset of Fig. 1 shows the characteristic LEED pattern of the clean FeO film taken at 60 eV.

The TDS spectra of EB from a well-ordered $Fe_3O_4(111)$ film are shown in Fig. 2. In addition to the α and β peaks, a broad distribution of chemisorbed EB labeled γ_1 appears which extends up to about 400 K. With increasing exposure the peak maximum temperature of γ_1-EB shifts from 400 K at very low exposure to 250 K. Upon higher exposure the γ_1 contribution continues to grow although the β peak begins already to form. We ascribe this deviation from sequential filling of sites to kinetic effects. Obviously, the equilibrium occupation of γ_1 and β sites is not established at the adsorption temperature of 100 K and not even during the TDS heating ramp. Both have saturated when the α peak appears after an exposure to about 2 L. An EB saturation coverage Θ_{sat} of 1 ML for β-EB—the same amount as on FeO(111)—and 0.9 ML for γ-EB can be derived by integration of the respective contributions in the 2 L curve. The desorption temperatures of α- and β-EB are the same as on FeO. At very high exposures (>4 L) the intensity in the β desorption range decreases indicating a decrease of the β-EB concentration. This is a hint that EB transforms from the physisorbed β to condensed α form by the influence of the thick EB multilayer. This is confirmed by the UPS results and will be discussed below.

The kinetic adsorption behavior is illustrated in Fig. 3 by the uptake curves $\Theta(\varepsilon)$ for the two investigated films at the adsorption temperature of 100 K. Shown is the β peak area from the TDS curves of FeO with its saturation value set to 1 ML and the sum of the $\beta+\gamma_1$ peak areas of Fe_3O_4, respectively. The desorption of the condensed α species (onset marked by arrows) starts only after the $\beta+\gamma_1$ layer has reached saturation.

The sticking coefficient $S=d\Theta/d\varepsilon$ is constant almost up to saturation. This implies the existence of a mobile precursor state on top of the physisorbed species. At 100 K both the adsorbed γ_1 and β species are immobile as concluded from the fact that they are not filled sequentially. The plot of the

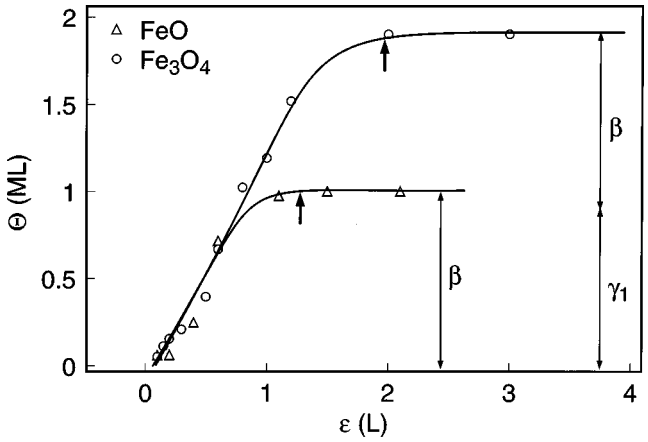

FIG. 3. Uptake curves coverage Θ vs exposure ε for EB on FeO(111) and $Fe_3O_4(111)$ films at 100 K. The coverage is evaluated from the areas of the corresponding TDS peaks. The saturation coverage of β-EB on FeO is attributed to 1 ML. The arrows indicate the exposure where the peak of condensed α-EB starts to develop.

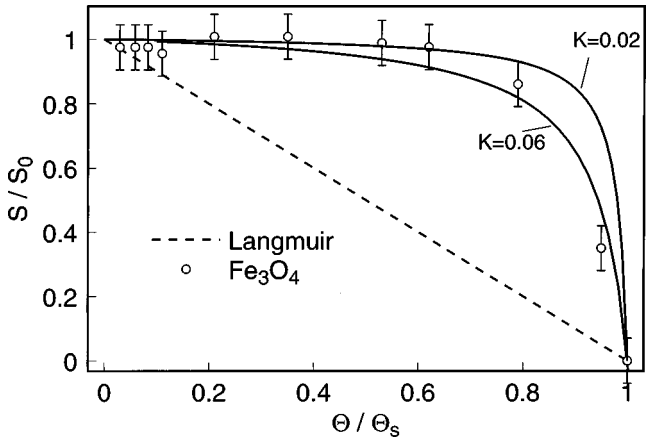

FIG. 4. Relative sticking coefficient S/S_0 vs relative coverage Θ/Θ_{sat} for the data of Fe_3O_4 shown in Fig. 3. The solid lines represent fits to the data points according to the theory of Kisliuk (Refs. 15, 16) for an adsorption kinetics with mobile precursor. The dashed line would be expected for Langmuir like behavior without mobile precursor.

relative sticking coefficient S/S_0 versus the relative coverage $\Theta_{\beta+\gamma 1}/\Theta_{sat}=n$ is shown in Fig. 4 for the Fe_3O_4 film. It is obvious that this adsorption behavior does not obey a Langmuir kinetics $S=S_0(1-n)$. The adsorption kinetics via a mobile precursor was introduced by Kisliuk[15,16]

$$S=S_0\left(1+\frac{n}{1-n}K\right)^{-1}.$$

Fits of the plot based on this formula yield a value for the constant

$$K=\frac{P_d'}{P_a+P_d}$$

between 0.06 and 0.02. Here, P_a is the probability of a precursor molecule on an empty site (intrinsic precursor) to transform into the chemisorbed state and P_d is the probability to desorb. P_d' is the probability of a precursor molecule on an occupied site (extrinsic precursor) to desorb. The probabilities for migration which compete with adsorption and desorption do not appear in the kinetics. At the exposure temperature of 100 K, the sticking coefficient is near unity which means that $P_a\cong 1$ and $P_d\cong 0$. The low observed value of K is therefore due to a low value of $P_d'\cong 0.02$ to 0.06. The competing migration probability of the precursor on occupied sites must thus be 0.94 to 0.98 which implies high mobility.

The uptake curve for α-EB (not shown) is always linear without saturation. This is typical for condensation which confirms that α peak is caused by condensed EB multilayer on the surface.

In order to determine the desorption energy E_{des} and the frequency prefactor ν, we start from the Polanyi–Wigner equation which gives the desorption rate R_i of molecules for a single adsorption state i with initial coverage Θ_i

$$R_i(T,\Theta_i(T_0))=-\frac{dn}{dt}=\nu(n)\exp\left[\frac{-E_{des}(n)}{k_BT}\right]n^x, \qquad (1)$$

and calculate

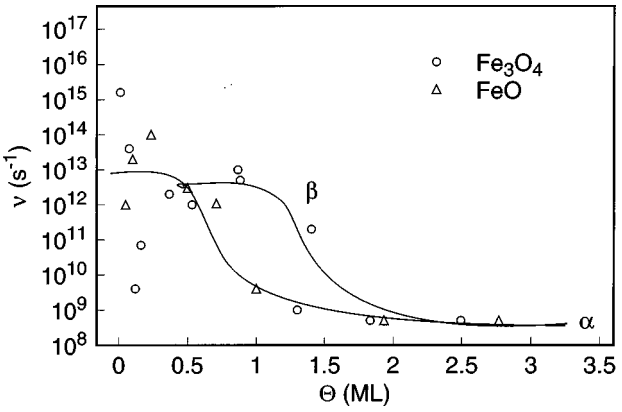

FIG. 5. Dependence of the frequency prefactor for desorption of EB from FeO and Fe_3O_4 films deduced from a threshold analysis of the TDS data.

$$\ln\left[\frac{-\frac{dn}{dt}}{n^x}\right]=\ln[\nu(n)]-\left[\frac{E_{des}(n)}{k_BT}\right]. \qquad (2)$$

T_0 and n are the adsorption temperature and the fraction of occupied adsorption sites and x is the reaction order for desorption. A plot of the left-hand side of Eq. (2) versus $1/T$ gives straight lines with the desorption energy E_{des} as slope and the logarithm of the frequency prefactor ν as intercept for each TDS spectrum if E_{des} and ν are not functions of coverage. In case of coverage dependence of E_{des} and ν the interpretation of the plot is no longer straightforward and the calculation can only be done with the first few percent of the TDS trace where the coverage can be considered as constant (threshold analysis).[17] The order x for the desorption of the condensed species α equals zero resulting in a coverage independent desorption rate. Equation (2) becomes more simple and the calculation of E_{des} and ν is easy. The mean values for the desorption energy $E_{des,\alpha}$ and the frequency prefactor ν_α are 44 kJ/mol and 5×10^{-8} s^{-1}, respectively.

The plot of the desorption energies versus coverage for the well-ordered FeO and Fe_3O_4 films are shown in Fig. 10(a). On FeO, the initial desorption energy for β-EB is constant at 55 kJ/mol. Beyond 1 ML it decreases abruptly to 44 kJ/mol, the value for condensed α-EB. On Fe_3O_4 the initial desorption energy is higher than: 90 kJ/mol and decreases with increasing coverage to the same value of 55 kJ/mol as found for β-EB on FeO. Also the final value for α-EB is the same as on FeO. As discussed above, the equilibrium distribution among β- and γ_1-EB on Fe_3O_4 is not established and the β state starts to be occupied long before the γ_1 contribution saturates. Since desorption at the threshold is then dominated by β-EB desorption, the drop of E_{des} in Fig. 10(a) does not mark γ_1 saturation coverage. This is different for the transition from β- to α-desorption energies. Desorption of α-EB does not start before saturation of $\beta+\gamma_1$ (see Fig. 3).

The coverage dependence of the frequency prefactors of the well-ordered films is shown in Fig. 5. The values scatter considerably but the general shape of the curves is similar to those of the desorption energies. This is called compensation effect[18] and has been observed frequently.

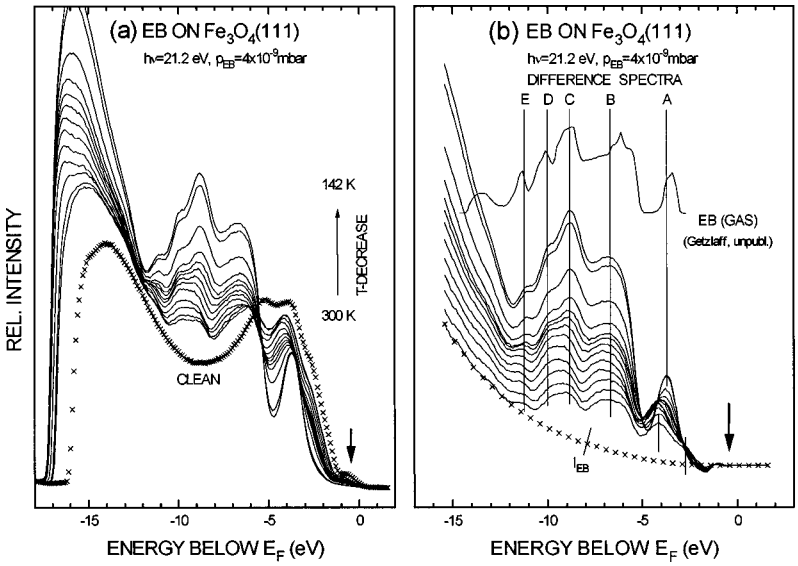

FIG. 6. (a) Photoelectron spectra of clean Fe_3O_4(111) and covered with EB in adsorption–desorption equilibrium at a constant pressure $p_{EB}=4\times10^{-9}$ mbar and constant temperatures between 300 and 142 K. (b) Difference spectra (covered minus clean) of the spectra in (a). The attenuation factors for the clean surface spectrum have been adjusted to yield zero intensity of the difference spectra at the position marked by an arrow. The spectra are compared to the EB gas phase spectrum from Getzlaff (Refs. 21,22).

B. Photoelectron spectroscopy

1. Electronic structure and coverage determination

Figure 6(a) presents a set of He I excited photoelectron spectra for the Fe_3O_4(111) surface measured in adsorption–desorption equilibrium at a constant pressure of 4×10^{-9} mbar EB at sample temperatures between 300 and 142 K. For comparison, also the clean surface spectrum is shown. The spectra were taken at time intervals of 6 min, 3 min for establishing the new temperature and the new equilibrium coverage and 3 min for taking the spectra. Figure 6(b) shows the corresponding difference spectra obtained after subtraction of the clean substrate spectrum. Since the adsorbate layer reduces the substrate emission, an attenuation factor

$$\mathrm{AF}=I/I_0=\exp-(d/l_e) \tag{3}$$

has to be applied to the substrate spectrum before subtraction (I_0, I: substrate intensity of the clean and the covered substrate; d: adsorbate thickness; $l_e=\lambda_e\cos\theta$ with λ_e=electron mean free path in the adsorbate layer and θ=mean escape angle of the electrons from the sample; for the used analyser $\theta=42°$). The only region in the spectrum where the adsorbate has no emission is the shoulder between 0 and about -1.5 eV in Fig. 6(a) which originates from Fe^{2+} related emission.[19,20] We adjust the attenuation factor AF so that the difference spectra become zero at the position indicated by an arrow at -0.4 eV. Using Eq. (3), values for $d/l_e=\ln(1/\mathrm{AE})$ are calculated which are proportional to the coverage.

The difference spectra in Fig. 6(b) show the features of molecularly adsorbed EB. This is demonstrated by comparison with the gas phase spectrum taken from references.[21,22] There is a 1-to-1 correspondence between the gas phase spectrum and the high-coverage EB spectra both concerning most peak positions and relative peak intensities. The main difference is the broadening of the adsorbate spectra which is commonly observed in adsorbate spectra and is due to the reduced life time of the excited states in the condensed relative to the gas phase.

At low coverage the spectra of the chemisorbed γ_1-EB are modified indicating stronger interaction with the surface. The most evident difference is the changed shape and position of the highest lying molecular orbital(s) (A). The main peak is shifted from -3.7 eV for the thick layer to -4.1 eV for initial adsorption. There is also a weak shoulder at -2.7 eV. Since also He II spectra show the same feature we attribute it to the highest occupied orbital in chemisorbed EB. Peak (A) originates from the highest lying occupied π orbitals of the phenyl group. In benzene it is degenerate. In EB the degeneracy is lifted but the split is small and causes only a broadening in the gas phase emission peak which is too small to be observable in the adsorbate spectra. That just this peak is most strongly modified in the low coverage spectra indicates that EB interacts with the surface via the π-electron system of the phenyl group. Therefore, we believe that it is lying flat. Similar peak shifts have been observed for benzene adsorbed both on metal surfaces[23–25] and oxides[26,27] and have been interpreted similarly. Also the shape and position of the other peaks in the low coverage spectra are modified. Especially we would expect a change in the lowest lying π orbital of the phenyl group. However, it overlaps with other orbitals both of the phenyl and the ethyl group which together form peak (B) and therefore cannot be separated. Since the general shape of the initial adsorbate spectrum still is similar to the gas phase spectrum, we conclude that also initial adsorption is molecular. A more detailed analysis will be published elsewhere.[28]

On the FeO(111) film the chemisorbed γ_1 phase is missing. Adsorption starts at a lower temperature and the UP spectra (not shown here) for initial adsorption (β-EB) and

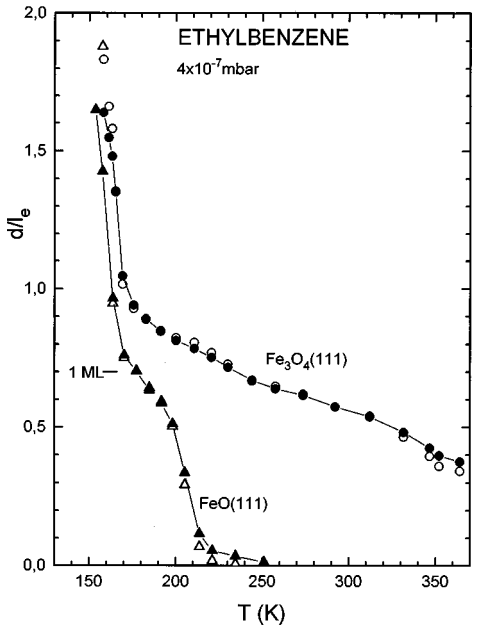

FIG. 7. Adsorption isobars: coverage vs T for 4×10^{-7} mbar EB on FeO and Fe_3O_4. Open symbols: coverage d/l_e in terms of adsorbate thickness d in units of the electron escape depth l_e as obtained from the attenuation factors for difference spectra formation. Full symbols: coverage as deduced from the adsorbate induced intensity in the photoelectron spectra and adjusted to d/l_e around $d/l_e=0.7$ (1 ML).

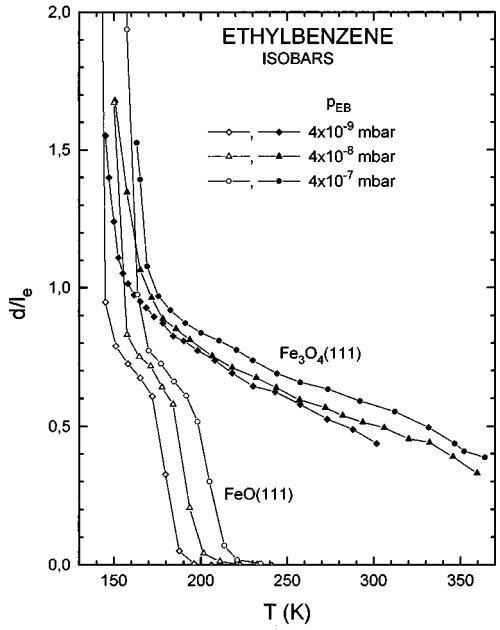

FIG. 8. Adsorption isobars: coverage (in terms of d/l_e) vs T as in Fig. 7 for different EB pressures as indicated.

the thick condensed layer (α-EB) are almost identical and correspond to the thick layer spectra on Fe_3O_4 in Fig. 6.

At least below 1 ML coverage, the area of the adsorbate induced features I_{EB} is a measure for the coverage. Beyond 1 ML, the increase of I_{EB} is smaller because of self-absorption in the adlayer. We first subtract the inelastic background from the difference spectra using an empirical curve [crosses in Fig. 6(b)]. Then the area marked I_{EB} is integrated. The contribution of peak (A) is not included in the integration because it is most strongly changed when going from chemisorbed to physisorbed EB.

We thus have two independent measures for the coverage: d/l_e and I_{EB}. We can use this to check the long-time stability of the spectrometer. An increase of spectrometer sensitivity would directly increase the intensity of the spectra and thus I_{EB}. The attenuation of the clean surface spectra before subtraction would have to be chosen smaller leading to a too large attenuation factor $AF=I/I_0$. However, inspecting Eq. (3), this causes an apparent *decrease* of d/l_e. The factor adjusting I_{EB} to d/l_e would change. We have used this countercurrent influence of a sensitivity change on the two independent measures for the coverage I_{EB} and d/l_e to correct the data if necessary.

2. Isosteric heat of adsorption

In Fig. 7 the isobars for $p_{EB}=4\times10^{-7}$ mbar for the two investigated films are compared. The open symbols represent d/l_e values. The filled symbols are I_{EB} values, adjusted to the d/l_e values in the region 0.5–1. It is evident that I_{EB} and d/le agree very well almost over the whole coverage range which proves that the valence emission intensity I_{EB} is a suitable measure for coverage. Only in the high coverage region, I_{EB} gives too low values as expected when multilayer adsorption occurs.

Even beyond 350 K, adsorption on Fe_3O_4 is considerable. The species in the region up to $d/l_e\cong0.55$ ($T\cong315$ K at this pressure) is chemisorbed (γ_1) and is represented by the low coverage spectra in Fig. 6. Below 320 K, the coverage continues to increase almost linearly. The corresponding spectra look very much like those of condensed EB but transition to condensation seems to occur only below about 170 K where the curve increases strongly. However, even beyond $d/l_e=2$, an equilibrium coverage can be established which means that the adsorption enthalpy still depends on coverage, although very weakly. Condensation with constant condensation energy and zero-order kinetics is thus not yet reached there.

The isobar for EB adsorption on FeO(111) shows no adsorption above 250 K. In agreement with the shape of the UP spectra, a chemisorbed species is missing. Below 220 K, the curve increases strongly with decreasing T, forms a shoulder at $d/l_e=0.65$ to 0.75 where obviously the physisorbed β-EB saturates before the transition to condensed α-EB occurs.

In order to derive isosteric heats of adsorption $q_{st}(\Theta)$, isobars were taken for three pressures as described in the experimental section. They are shown in Fig. 8. For each coverage Θ, a set of three $p-T$ pairs can be taken from the three isobars. According to the Clausius-Clapeyron equation,

$$\ln p=-[q_{st}(\Theta)/R](1/T)+\text{const.}, \tag{4}$$

the isosteric heat of adsorption $q_{st}(\Theta)$ can be deduced from the slope of the plots $\ln p$ over $1/T$, a few of which are shown in Fig. 9 for the case of adsorption on FeO. The three data points for each coverage fit quite well to a straight line which is also evident from the fact that the isobars in Fig. 8

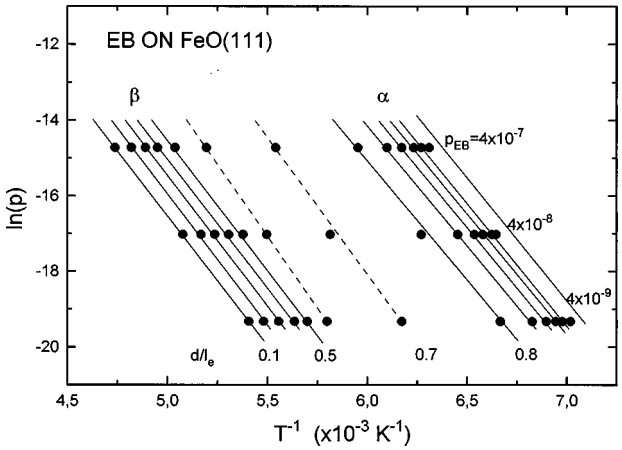

FIG. 9. $\ln p$ over T^{-1} for different coverages in terms of d/l_e given as parameters, taken from the data in Fig. 8.

are equidistant for all coverages. The deduced values $q_{st}(\Theta)$ are shown in Fig. 10(b) together with the corresponding values from $Fe_3O_4(111)$. For FeO, there are two regions in the $q_{st}(\Theta)$ curve. Up to $d/l_e=0.5$ (0.7 ML), q_{st} is constant (58 kJ/mol), then follow two values which seem too high and at $d/l_e\cong 0.7$ (1 ML) it decreases to a slightly lower final value of 53 kJ/mol. The initial and the final constant values correspond to the two steeply increasing parts of the isobars in Fig. 8 which we ascribe to physisorbed β- and condensed α-EB. In Fig. 9, the corresponding sets of lines are separated by a strong offset in the $1/T$ direction indicating a change in the adsorption kinetics. The data for $d/l_e=0.7$ are halfway between both sets. This coverage corresponds thus to the completion of the physisorbed layer. As in the TDS measurements we call this 1 ML.

We do not know why the q_{st} values in the transition region ($d/l_e=0.6,0.7$) are too high. The simplest explanation would be that the d/l_e scale for the three isobars in Fig. 8 differs due to variations in experimental sensitivity which we have not observed, however.

The isobars for Fe_3O_4 in Fig. 8 are equidistant in the low and in the high coverage region. In the intermediate range ($d/l_e\cong 0.6-1.0$), the isobar for 4×10^{-8} mbar which was measured with increasing T appears too low. If this were a consequence of not waiting long enough for establishment of adsorption–desorption equilibrium, we would just expect the opposite: The 4×10^{-9} mbar curve, measured with decreasing T should be too low and the 4×10^{-8} mbar curve measured with increasing T should be too high. Also the 4×10^{-9} and the 4×10^{-7} mbar curves, both measured with decreasing T, seem quite near together in that range. This leads to quite high values for q_{st} which even increase with coverage [Fig. 10(b)]. Therefore, we do not consider the q_{st} values as reliable in the transition region $d/l_e=0.6-1.0$. For low coverage, q_{st} comes down from a value around 85 kJ/mol which is a lower limit for chemisorbed γ-EB. Since we could not measure the isobars for $T>370$ K, we have no q_{st} values for $d/l_e<0.45$. The chemisorbed phase saturates at $d/le\cong 0.55$, corresponding to a coverage of almost 80% of the physisorbed β-EB saturation on FeO, i.e., 0.8 ML. At high coverage, q_{st} decreases to almost the same value of 52 kJ/mol as on FeO, corresponding to beginning condensation (α-EB). The coverage range of the intermediate region in Fig. 10(b) is just as wide as the thickness of the physisorbed β-EB on FeO. We conclude that adsorption of 1 ML of β-EB preceeds condensation irrespective of what is below (FeO substrate or chemisorbed γ_1-EB layer on Fe_3O_4). Different from the TDS measurements, the occupation of β and γ_1 sites occurs strictly sequentially in the equilibrium measurements.

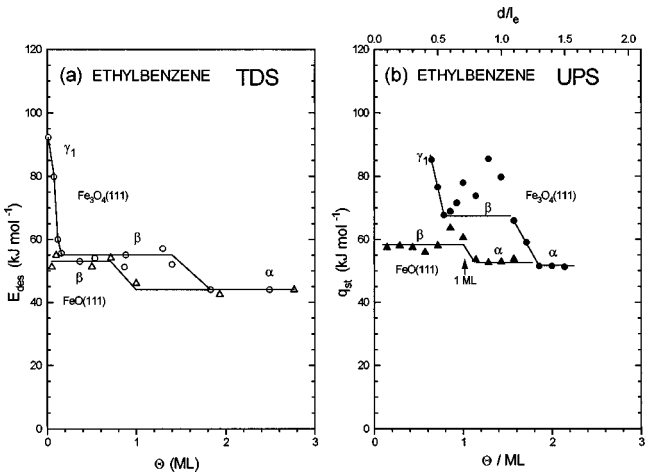

FIG. 10. (a) Coverage dependence of the desorption energy E_{des} for EB from FeO and Fe_3O_4 as derived from a thereshold analysis of the TDS data. (b) Coverage dependence of the isosteric heat of adsorption q_{st} for EB from FeO and Fe_3O_4 as derived from the slopes of the curves as in Fig. 9 using the Clausius–Clapeyron equation.

3. Work function change

As can be seen from the shift of the low energy onset of the spectra in Fig. 6, EB adsorption causes a strong decrease of the work function φ. The work function change $\Delta\varphi$ vs coverage d/l_e is plotted in Fig. 11.

On FeO, we observe an initial small decrease of about -0.05 eV within a very small coverage range. The reason for this is not known since the spectra are otherwise not changed apart from a slight increase of the background intensity. $\Delta\varphi$ then decreases more slowly to -0.25 eV when the physisorbed ML is completed. The following condensation is accompanied by a further decrease to a final value of about -0.53 eV. The curve is independent of the applied EB pressure and equal for measurement with decreasing and increasing T which indicates that equilibrium is established everywhere.

On Fe_3O_4 the initial decrease is very strong and linear and reaches a value of $\Delta\varphi=-1$ V when the chemisorbed γ_1-EB layer is completed at $d/l_e=0.55$ (0.8 ML). If we assume (as will be discussed below) that each EB molecule occupies two $Fe_3O_4(111)$ surface unit cells or about 61 Å^2, we can use the Helmhotz equation

$$\Delta\varphi=n\mu/\varepsilon_0, \tag{5}$$

to calculate the dipole moment $\mu_{\gamma1}$ per molecule in the γ_1 state (ε_0=dielectric constant, n=adsorbate density). We find

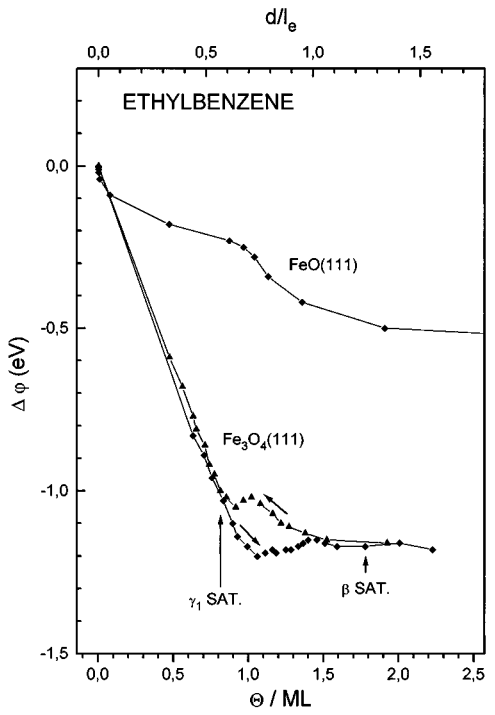

FIG. 11. Coverage dependence of the work function change $\Delta\varphi$ for EB adsorption on FeO and Fe_3O_4. For details see the text.

$\mu_{\gamma 1}=1.62$ D. (For comparison, the dipole moment of the free water molecule is 1.84 D.) This value indicates that the molecules are polarized considerably. The negative sign of $\Delta\varphi$, means that molecules are polarized with the positive side towards the vacuum and the negative side towards the substrate or that there even is a transfer of electronic charge from the adsorbate to the substrate. A comparable value of 2 D for the dipole moment has been observed for benzene adsorption on transition metals.[18]

Beyond 0.8 ML, the shape of the $\Delta\varphi$ curve depends on the direction of measurement and forms a hysteresis loop for $0.55<d/l_e<1.0$ ($0.8<\Theta<1.4$). This is the region where the corresponding isobars in Fig. 8 were not equidistant and too narrow together yielding unreliable and too high values for q_{st}. The shape of the $\Delta\varphi$ curve for decreasing d/l_e is similar to the shape of the FeO curve in the range $d/l_e>0.7$.

In line with the TDS observations, we interpret this behavior as follows. With increasing coverage, first the chemisorbed γ_1 layer is formed, on top of it the physisorbed β and finally the condensed α layer. When the condensed layer reached a certain thickness, the physisorbed layer transforms and adjusts its structure to the condensed layer. This starts probably around $d/l_e=0.7$ (1 ML) where the $T\downarrow$ measurement reaches its minimum. The transformation is finished around $d/l_e=1.0$ (1.4 ML), where the $T\downarrow$ and the $T\uparrow$ curves coincide. During the $T\uparrow$ measurement, the condensed layer desorbs. The last layer of it should convert back to β-EB. This is obviously kinetically hindered and desorption proceeds further. Only near $d/l_e=0.7$ (1 ML), the rest of it transforms back to physisorbed β-EB. Since the heat of adsorption for the condensed species is smaller, desorption proceeds ''too fast'' in the range $\Theta=1.4$ to 1 ML which leads to the too low lying 4×10^{-8} mbar isobar in Fig. 8. The coverage in this range is thus strongly influenced by the transformation kinetics between α- and β-EB and an equilibrium coverage is not established. Consequently, the q_{st} values are unreliable.

On FeO, no $\Delta\varphi$ hysteresis was observed. We are not sure whether the initial physisorbed layer transforms into condensed EB or not. The observed ''too high'' values for q_{st} in the transition region $d/l_e=0.6-0.7$ could be an indication that a similar effect occurs which, however, is so weak that no hysteresis is visible in the $\Delta\varphi$ curves.

4. Saturation coverages and surface structure

On FeO we found that the physisorbed layer saturates at $d/l_e\cong0.7$. If we assume that EB is lying flat on the surface and assume the same thickness $d=3.7$ Å as the van der Waals thickness of benzene,[29] we obtain [using Eq. (3)] a value for the electron mean free path $\lambda_e=6.5$ Å for the energy $E\cong20$ eV above the valence band edge. This is a reasonable value and compares well with tabulated data.[30]

Both TDS and UPS measurements show that the chemisorbed layer on Fe_3O_4 saturates at a coverage below 1 ML (0.9 ML in TDS, 0.8 ML using UPS). $Fe_3O_4(111)$ forms a 2×2 superstructure (cf. LEED pattern in Fig. 2 and Ref. 33). Its unit cell has an area of 30.4 Å^2. Constructing a van der Waals contour for EB from the molecular structure and the van der Waals radii of the atoms we find that the molecule area is about 50 Å^2. The interaction is strong and specific and it appears reasonable to assume that all molecules occupy identical sites. This would prevent a dense packing. Assuming that each molecule occupies two substrate (2×2) unit cells, saturation would occur at a coverage of $50/(2\times30.4)=0.82$ which fits reasonably well with the observed values.

Such a structure could give rise to a superstructure. Yet, no superstructure was observed in LEED. The reason could be that the 2D packing is strongly disturbed by unoccupied single (2×2) substrate unit cells. Rotational disorder of the adsorbed molecules is also likely.

IV. DISCUSSION

TDS measurements occur principally far from adsorption–desorption equilibrium. In order to guarantee a constant heating rate in the range where desorption occurs, the exposure is done at a considerably lower temperature. It is possible that an equilibrium distribution among different sites is not reached during adsorption if mobility is required or if adsorption is activated. The deviation from sequential filling of the γ_1 and β sites of EB on Fe_3O_4 illustrates this. In contrast, sequential filling is strictly fulfilled in the equilibrium measurements using UPS.

The desorption rate in TDS is determined by the desorption energy E_{des} and by details of desorption kinetics, expressed in the reaction order x and the frequency factor ν. If adsorption is activated, E_{des} contains this activation energy. Generally, $E_{\mathrm{des}}\geqslant q_{\mathrm{st}}$ should hold with the equality sign valid for nonactivated adsorption. The advantage of TDS measurements is that they are experimentally relatively simple, that

the method is generally applicable also in cases where the establishment of adsorption–desorption equilibrium is difficult or impossible (see below) and that the kinetic parameters x and ν can be determined.

A principal question in the measurements of adsorption isobars $\Theta(T)_{p=\text{const}}$ using UPS for the determination of Θ is whether thermodynamic adsorption–desorption equilibrium really is established. For this it is necessary that both adsorption and desorption are fast enough. For desorption this seems no problem. In order to check adsorption velocity, we have monitored the increase of the adsorbate signal upon a steplike increase of p_{EB}. The result was that the coverage increases quickly with a sticking coefficient near unity and saturates relatively sharply[28] which means that equilibrium is established within about 3 min even at the lowest applied pressure of 4×10^{-9} mbar. A further check is whether measurements with decreasing T (increasing Θ) and increasing T (decreasing Θ) yield identical isobars. For adsorption on FeO(111) this was always fulfilled. For $Fe_3O_4(111)$ this was not fulfilled in the coverage regime of the transition between physisorption (β-EB) and condensation (α-EB). As discussed above, this was not caused by too slow establishment of equilibrium coverage but by a structural transition of β-EB$\leftrightarrow\alpha$-EB which obviously is slow or inhibited.

The coverage has been determined in two ways by UPS. The determination of d/l_e from the substrate signal attenuation needs a region in the spectrum where no other adsorbate induced changes occur. This was given in a narrow range below the valence band edge. A small adsorbate induced change of substrate emission was observed on Fe_3O_4 around -1.8 eV and induced a minimum in the difference curves [see Fig. 6(b)]. Between 0 and -1 eV, however, no such effects were observed. When deducing the coverage from adsorbate induced emission (I_{EB}), difficulties may arise if the nature of the adsorbate or its orientation depends on coverage. To minimize these influences we have not used the spectral range where strong variations are observed, i.e., the range of the topmost π orbitals. Orientation effects are minimized by the use of an angle integrating spectrometer. The crucial check, however, is that the isobars using d/l_e and I_{EB} coincide (Fig. 7).

Further, the adsorbate must not be influenced by the irradiation which was checked. If different species as, e.g., dissociated and undissociated species would exist simultaneously, a separation would be difficult. Above about 400 K, slow spectral changes were observed on a time scale of about 30 min which possibly originate from dissociation. This limited the UPS determination of the coverage to $T<400$ K whereas TDS principally is possible even then as long as desorption again is molecular.

An advantage of the equilibrium measurements is the observation of strictly sequential saturation of the γ_1 and β species on Fe_3O_4. The drop of q_{st} in Fig. 10(b) at 0.8 and 1.8 ML, respectively, gives therefore reliable saturation coverages for γ_1- and $(\gamma_1+\beta)$-EB.

Table I compares the values E_{des} deduced from TDS with q_{st} deduced from the equilibrium measurements. For γ_1, the initial value of 91 kJ/mol from TDS fits well with the values from the equilibrium measurements which drop from 85 to below 70 kJ/mol with increasing coverage assuming a repulsive lateral interaction. A repulsive interaction is also in agreement with the wide range of γ_1 desorption in TDS (Fig. 2). Also the values for β-EB agree ($E_{\text{des}}=55$ kJ/mol, $q_{\text{st}}=58$ kJ/mol for FeO; determination of q_{st} for Fe_3O_4 was not possible). The agreement means that adsorption of γ_1- and β-EB is not activated. The agreement for condensation (α-EB) is not so good, however. E_{des}(44 kJ/mol)is clearly lower that q_{st}(52 kJ/mol). The possible reason may be that the condensate in the TDS experiments was strongly disordered (maybe even dendritic or glasslike) due to the low adsorption temperature (100 K) with correspondingly lower E_{des}. The applied threshold analysis considers only the molecules desorbing first which may be bound more loosely. In former experiments the adsorption of EB was carried out at 120 K.[8] The value of E_{des} derived from these data was 50 kJ/mol which fits quite well with the value of q_{st} measured here. In the equilibrium measurements, the coverage was T dependent even for coverages well above 3 ML which means that the reaction was not yet of zero order as would be expected for condensation. Obviously even then the absorbate ''feels'' the substrate and is slightly more tightly bound than in the condensate. The correct heat of condensation is probably around 50 kJ/mol.

TABLE I. Desorption energies E_{des}, isosteric heats of adsorption q_{st}, frequency prefactors ν for desorption and saturation coverages for chemisorbed γ_1-EB (chemisorbed), β-EB (phsisorbed) and α-EB (condensed) on FeO(111) and $Fe_3O_4(111)$ surfaces as determined by TDS and UPS measurements.

		TDS		UPS	
		FeO	Fe_3O_4	FeO	Fe_3O_4
α	E	$E_{\text{des}}=44$ kJ/mol[a] 50 kJ/mol[b]		$q_{\text{st}}=52$ kJ/mol	
	ν	5×10^{8} s^{-1}		...	
β	E	$E_{\text{des}}=55$ kJ/mol		$q_{\text{st}}=58$ kJ/mol	
	ν	5×10^{12} s^{-1}		...	
	Θ_{sat}	1 ML		1 ML	
γ_1	E	...	$E_{\text{des}}=91$ kJ/mol	...	$q_{\text{st}}=85$ kJ/mol
	ν	...	2×10^{15} s^{-1}	...	...
	Θ_{sat}	...	0.9 ML	...	0.8 ML

[a]This work, adsorption temperature 100 K.
[b]Reference 8 adsorption temperature 120 K.

The UP spectra both in the α- and β-EB range in Fig. 6(b) are very similar to the EB gas phase spectrum as expected for condensed and physisorbed EB. The FeO curve in Fig. 11 shows that the related work function changes are not very large and thus the polarization of α- and β-EB is not very strong. The UP spectrum of γ_1-EB, however, is more strongly affected, especially in the highest π-orbital range. These orbitals correspond to the $1e_{1g}$ orbitals in the benzene which have a large spatial extension out of the plane of the aromatic ring. A shift of the $1e_{1g}$ orbital towards higher binding energy has been observed upon adsorption and has been interpreted as due to the strong interaction with the substrate when benzene is lying flat on the surface.[23–27] Because of the very similar behaviour we believe that also

γ_1-EB is lying flat on the surface. The high polarization induced dipole moment of 1.62 D which we have found supports this.

On FeO(111), no chemisorbed γ_1-EB was observed. According to Refs. 31 and 32, this surface is oxygen terminated. $Fe_3O_4(111)$, on the other hand, is iron terminated with $\frac{1}{4}$ ML of Fe atoms in the topmost layer.[33] We ascribe the existence of γ_1-EB to the interaction of EB with the metal (iron) atoms in the first layer. This is supported by the observation of a similar strongly bound species on the pure Pt(111) surface.[28] Insofar, the EB absorption measurements confirm the surface structure models for $FeO(111)$[31,32] and $Fe_3O_4(111)$.[33]

V. SUMMARY

The adsorption of ethylbenzene (EB) on well ordered epitaxial FeO(111) and $Fe_3O_4(111)$ films was studied with TDS, UPS, and LEED. The UPS measurements were performed under adsorption–desorption equilibrium conditions. The equilibrium measurements using UPS and the nonequilibrium measurements using TDS are complementary. UPS probes the species in the adsorbed state, TDS probes what is coming off the surface. Only molecular species were observed.

Three species are identified both by UPS and TDS: chemisorbed γ_1-, physisorbed β-, and condensed α-EB. They are distinguished by their peak position and shape in TDS, by their different UP spectra and by their different desorption energies E_{des} and isosteric heats of adsorption q_{st}. On the FeO film which is O terminated, physisorbed β-EB adsorbs first, followed by condensation. The chemisorbed γ_1-EB exists only on the Fe_3O_4 surface which contains Fe atoms in the top layer indicating a strong metal–EB interaction. From the shift and split of the topmost phenyl derived π orbitals in UPS we conclude that the phenyl ring lies flat on the surface. Defining the saturation coverage of the physisorbed β-EB as 1 ML, the γ_1 phase saturates at about 0.8 ML. On top of it, 1 ML of physisorbed and finally condensed EB is observed. Under the influence of the condensed layer, the physisorbed intermediate layer converts to condensed EB, too.

Desorption energies E_{des} and isosteric heats of adsorption q_{st} agree well indicating that no (or only small) activation barriers for adsorption exist. Values for E_{des} and q_{st}, respectively, are 91 and 85 kJ/mol for γ_1-EB (coverage dependent), 55 and 58 kJ/mol for β-EB, and 50/44 (depending on adsorption temperature) and 52 kJ/mol for α-EB.

In the equilibrium measurements, γ_1- and β-EB adsorb strictly sequentially. At the low adsorption temperature of 100 K used for the TDS measurements, adsorption of β-EB starts long before γ_1 saturation indicating insufficient mobility. However, the common precursor state for them is mobile and follows a Kisliuk kinetics.

[1] E. H. Lee, Catal. Rev. **8**, 285 (1973).
[2] T. Hirano, Appl. Catal. **26**, 65 (1986).
[3] T. Hirano, Appl. Catal. **28**, 119 (1986).
[4] M. Muhler, J. Schütze, M. Wesemann, T. Rayment, A. Dent, R. Schlögl, and G. Ertl, J. Catal. **126**, 339 (1990).
[5] M. Muhler, R. Schlögl, and G. Ertl, J. Catal. **138**, 413 (1992).
[6] W. P. Addiego, C. A. Estrada, D. W. Goodman, M. P. Rosynek, and R. G. Windham, J. Catal. **146**, 407 (1994).
[7] K. Coulter, D. W. Goodman and R. G. Moore, Catal. Lett. **31**, 1 (1995).
[8] D. Zscherpel, W. Weiss, and R. Schlögl, Surf. Sci. **382**, 326 (1997).
[9] W. Ranke, Surf. Sci. **342**, 281 (1995).
[10] W. Weiss, Surf. Sci. **377**, 943 (1997).
[11] W. Weiss, M. Ritter, D. Zscherpel, M. Swoboda, and R. Schlögl, J. Vac. Sci. Technol. A **16**, 21 (1998).
[12] M. Ritter, W. Ranke, and W. Weiss, Phys. Rev. B **57**, 7240 (1998).
[13] R. L. Summers, Lewis Research Center, NASA Technical Note TN D-5285, Washington, D.C. (1969) (distributed by VARIAN).
[14] U. Scheithauer, G. Meyer, and M. Henzler, Surf. Sci. **178**, 441 (1986).
[15] P. J. Kisliuk, J. Phys. Chem. Solids **3**, 95 (1957).
[16] P. J. Kisliuk, J. Phys. Chem. Solids **5**, 78 (1958).
[17] E. Habenschaden and J. Küppers, Surf. Sci. **138**, L147 (1984).
[18] G. A. Somorjai, *Introduction to Surface Chemistry and Catalysis* (Wiley-Interscience, New York, 1994).
[19] R. J. Lad and V. E. Henrich, Phys. Rev. B **39**, 13478 (1989).
[20] Th. Schedel-Niedrig, W. Weiss, and R. Schlögl, Phys. Rev. B **52**, 17449 (1995).
[21] M. Getzlaff (unpublished).
[22] M. Getzlaff and G. Schönhense, Surf. Sci. **377–379**, 187 (1997).
[23] J. E. Demuth and D. E. Eastman, Phys. Rev. Lett. **32**, 1123 (1974).
[24] G. L. Nyberg and N. V. Richardson, Surf. Sci. **85**, 335 (1979).
[25] P. Hofmann, K. Horn, and A. M. Bradshaw, Surf. Sci. **105**, L260 (1981).
[26] G. W. Rubloff, H. Lüth, and W. D. Grobman, Chem. Phys. Lett. **39**, 493 (1976).
[27] H. Raza, P. L. Wincott, G. Thornton, R. Casanova, and A. Rodriguez, Surf. Sci. (to be published).
[28] W. Ranke and W. Weiss (unpublished).
[29] A. J. Gordon and R. A. Ford, *The Chemists Companion* (Wiley, New York, 1972).
[30] M. P. Sea and W. A. Dench, Surf. Interface Anal. **1**, 2 (1979).
[31] C. S. Fadley, M. A. Van Hove, Z. Hussain, and A. P. Kaduwela, J. Electron Spectrosc. Relat. Phenom. **75**, 273 (1995).
[32] H. C. Galloway, P. Sautet, and M. Salmeron, Phys. Rev. B **54**, R11145 (1996).
[33] W. Weiss, A. Barbieri, M. A. Van Hove, and G. A. Somorjai, Phys. Rev. Lett. **71**, 1848 (1993).